Proc. of the 9th Intl. Conf. of Asian Society for Precision Engg. and Nanotechnology (ASPEN 2022)
15–18 November 2022, Singapore. Edited by Nai Mui Ling Sharon and A. Senthil Kumar
doi://10.3850/978-981-18-6021-8_OR-12-0064

Generation of Micro Lenslet Arrays using High Efficiency Synchronized Diamond Milling

Nicholas Yew Jin Tan #, Rui Huang, Dennis Wee Keong Neo, Kui Liu
Singapore Institute of Manufacturing Technology, 71 Nanyang Drive, Singapore 638075, Singapore
Corresponding Author / Email: nicholas_tan@simtech.a-star.edu.sg, TEL: +65-9617-1286

KEYWORDS: Functional Surfaces, Micromilling, Ultra-precision, Optical

With functional surfaces gaining much attention due to their ability to effectively and passively enhance the performance of the components that they are coupled with, the need for high efficiency fabrication techniques is needed to be able to meet the demands of the industry. However, current fabrication techniques for micro lenslet arrays are relatively slow, especially so for planar surfaces. The fine diamond tips used in Single Point Diamond Turning requires the tool to travel long cutting distances to cover the surface, despite using enabling technologies like the fast tool servo. Diamond milling on the other hand is slow due to the need for tool indexing at each position. This introduces non-productive time into the process, reducing the overall efficiency of fabricating lens arrays. High Efficiency Synchronized Diamond Milling (HESDM) avoids much of the non-productive indexing time by leveraging on the high frequency duty cycle of the milling spindle. With a reciprocating workpiece, the relative motions would allow for synchronous machining and indexing of micro lenslets, producing them at high speeds. Thus, in this study, the parameters that influence the generated features are studied, producing a micro lens array mold using the HESDM process.

NOMENCLATURE

β = Tilt angle
D = Depth-of-Cut (DoC)
D_c = Critical DoC
F = Reciprocating Workpiece Feed
L = Length of Lenslet
N = Rpm
r_t = Milling tool radius
S = Inter-lenslet Spacing
T_{on} = On-duty cycle
T_{off} = Off-duty cycle
W = Width of Lenslet

1. Introduction

With the advent of digitalization and automation changing the manufacturing industry, there is a pressing demand for the need of high-quality optics to increase the effectiveness of the various optoelectronic sensors deployed today. Pyroelectric sensors for example use an infrared signal to trigger an electric signal, allowing for automatic activation of various devices when a heat source is detected [1]. Such sensors have seen wide application, especially in energy-saving systems which only activate upon the detection of human presence nearby. However, such sensors do not possess great spatial coverage, only detecting sources perpendicularly to its surface. As such, lenses are always used in conjunction with these sensors to passively increase the overall practicality of the device, instead of deploying multiple sensors.

Currently, mass replication techniques are used to provide high throughput of such lenses. As characteristics of the optical elements produced by such techniques heavily reliant on the quality of the mold features, it is necessary to produce these molds with excellent geometrical accuracy and superior surface finish. This is to ensure the effective deployment of these lenses without compromising on the optical performance. Single Point Diamond Turning (SPDT) using Ultra-Precision Machining (UPM) has been the go-to processing technology for the fabrication of such optical elements, being able to meet the stringent demands required for these lenses [2]. With the rapid development in UPM research, highly complex and intricate features can now be machined with the aid of multi-axial stage positioning [3-5].

However, due to the nature of SPDT, the efficiency in the production of such functional surfaces is limited, affecting the overall throughput of these functional surfaces. The introduction of the Fast-Tool Servo (FTS) has allowed for high-frequency low-amplitude modulation of the machined depth, allowing for faster processing of functional surfaces like micro lenslet arrays [6]. Nevertheless, the processing speed is limited to the positioning ability of the FTS, along with the frequency of the features at the extremities of the component.

Another alternative to produce lenslet arrays is by micromilling. While this processing technique is flexible in terms of the types of surfaces it can produce the lenslets on, it is comparatively inefficient to FTS processes due to the excessive need for non-productive indexing of the tool. Furthermore, the tip of the tool possesses a zero-velocity zone along the spindle axis, affecting the optical quality of the lens at the apex of the feature.

As such, in this paper, we propose a novel High Efficiency Synchronized Diamond Milling (HESDM) technique to produce large micro lenslet arrays. This technique leverages on the high rotational speed of a milling spindle, along with a small radius of gyration, to create lenslets at high feeds using the relative physical interactions between the tool and the workpiece. By tilting the tool at an angle relative to the contact tangent of the workpiece, not only are the zero-velocity zones avoided during the machining process, but the tool-workpiece interaction is no longer continuous, allowing for indexing of the contact locations with a continuous feed instead of non-productive indexing motions.

2. High Efficiency Synchronized Diamond Milling

2.1 Principle of HESDM

The principle of the HESDM process requires the use of a milling spindle with a tilted tangent to the surface of the workpiece. This tilted position firstly steers the zero-velocity zone aways from the tool-workpiece interaction, allowing for the lenslets to be machined with better surface quality using the higher velocity sectors of the tool's rake, as seen in Fig. 1. Furthermore, an on-off duty cycle can be observed when the depth-of-cut (DoC), D, smaller than a critical value, D_c, of the tool radius, as follows:

$$D < D_c = r_t(1 - \cos\beta) \quad (1)$$

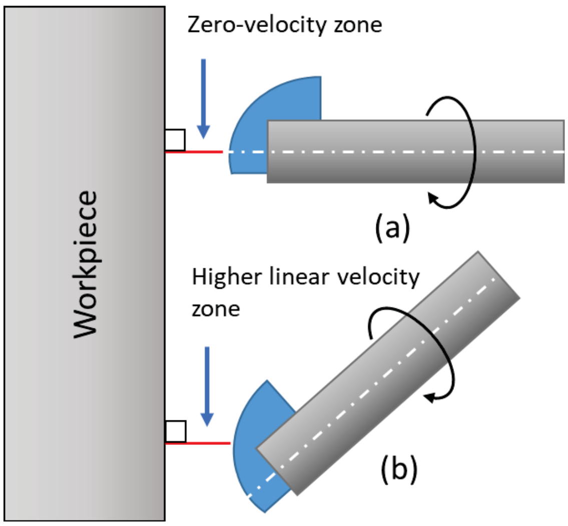

Fig. 1 Linear velocity of milling tool along the rake face depending on angular position (a) conventional perpendicular (b) Diagonally aligned

Where r_t is the radius of the milling tool and β is the tilt angle of the spindle axis with respect to the tangent of the workpiece surface. This duty cycle can be determined based on the geometrical interactions between the tool and workpiece, based on the working parameters. Using time as a unified reference, the on and off duty cycle, T_{on} and T_{off}, can be determined as follows:

$$T_{on} = \frac{2\sin^{-1}\left(\frac{0.5W}{r_t}\right)}{6N} \quad (2)$$

$$W = 2\sqrt{r_t^2 - (r_t - D)^2} \quad (3)$$

$$T_{off} = \frac{60}{N} - T_{on} \quad (4)$$

Where N is the rpm of the spindle. The lenslet width, W, is reflection of the interference between the contact of the tool and the workpiece, defined by the DoC. Using this notion, the tool is in contact with the workpiece during the on-duty cycle and is indexing to the next location during the off-duty cycle of the process. This is done using a reciprocating workpiece with a relative linear motion, allowing for the lenslet generation and the indexing of each lens to be done in a continuous fashion, as shown in Fig. 2. As the feed is constant for both the on and off cycles, the length of each lenslet, L, and the corresponding spacing between the apex of each lenslet, S, can be determined as follows:

$$L = T_{on}\left(\frac{2\pi N r_t \pm F}{60}\right) \quad (5)$$

$$S = F/N \quad (6)$$

Where L is the length of the lenslet and F is the reciprocating feed of the tool, where the positive notion is used when moving against the rotation of the tool.

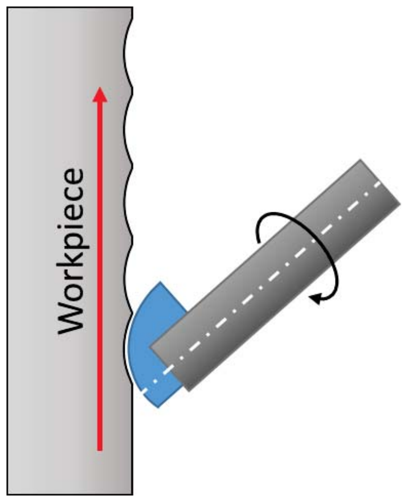

Fig. 2 High efficiency generation of micro lenslet with HESDM technique, avoiding the need for non-production indexing motion.

2.2 Lenslet Distribution

From the derived equations, it can be observed that the feed of the reciprocating workpiece not only affects the length of the lenslets, but also the spread of them as well. As such, the distribution of the lenslets is tough to visualize due to the convoluted relationship between the many parameters. To address this issue and provide a clearer picture on the interactions between the parameters, a graphical representation of the machined lenslet spread was developed using numerical tools, as shown in Fig. 5.

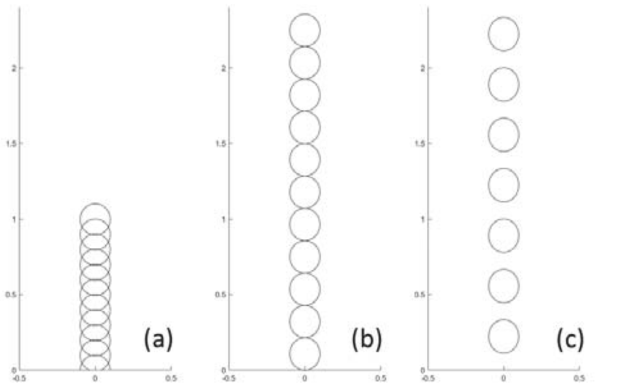

Fig. 5 Spread of lenslets with varying reciprocating feeds. (a) Low reciprocating feeds resulting in feature overlap. (b) Side-by-side feature distribution with maximum fill factor over the length at critical feed value. (c) High reciprocating feed resulting in spaced distribution of lenslets.

From Fig. 5(a) it can be observed that at low feeds, the tool-workpiece interaction is like that of conventional milling material removal. As the reciprocating feed is slow, the generated features will overlap, creating a groove instead of discrete lenslets. On the other extreme end in Fig. 5(c), the high feed of the reciprocating workpiece will result in the lenslet features spread far apart, not fully utilizing the entire length of the machined area. There thus lies a sweet spot where the reciprocating feed will result in the length of the lenslet and the spread to be very close, maximizing the machined area with the desired lenslet array with minimal spread.

To identify this critical point, the relationship between the lenslet length and the spread can be plotted with each other against varying feeds. By fixing the DoC, tool radius, and the rpm of the tool, an optimality for maximum fill-factor can be identified via the intercept of both plots, as shown in Fig. 3, reducing the complexity of the multivariable relationship. As such, the optimal feed and characteristic length of the lenslet achievable with the other fixed parameters can be obtained.

Using this result, each rpm parameter results in a single recommended reciprocating feed, which also possesses a characteristic length. As the machining parameters have a linear relationship with the characteristic length, they can be plotted with each other, as seen in Fig. 4. The upper limit of the plot is set to the maximum feed of the translation axis used in this process. It can be easily observed that the optimal characteristic length of the lenslets produced by this technique settles at a minimal value, of which is still slightly larger than the width of the lens. This is due to the relative non-zero motion required for the continuous generation of the lenses,

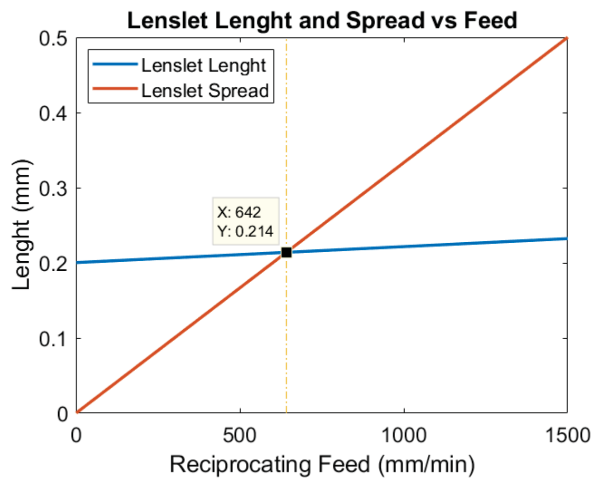

Fig. 3 Identifying the intercept point to obtain the characteristic lenslet length and feed for maximum fill-factor with a 3000-rpm tool with a 0.5mm radius.

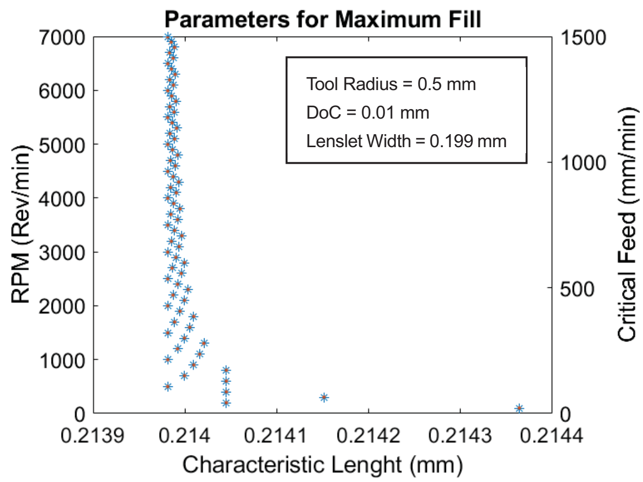

Fig. 4 Characteristic lenslet length and the corresponding machining parameters required to generate it.

requiring the tool to contact the workpiece over a slightly longer distance compared to stationary milling. This produces near-spherical toric lenses which have anisotropic focal performance, increasing the functionality of the surface. As such, using the chart would allow one to easily determine the required machining parameters for the desired achievable lenslet length at the feature DoC to obtain a machined surface with maximum fill-factor to optimize the area functionality.

2.3. Experimental Setup

The experiment was conducted in a five-axis ultra-precision machine, with an additional high speed milling spindle attachment, as shown in Fig. 6. The tool used was a conventional 0.5 mm radius single flute diamond mill, with a 24 mm by 24 mm by 11 mm thick aluminum workpiece set upon the spindle. The workpiece was firstly trimmed using a conventional 0.2 mm radius diamond tool to prepare and flatten the workpiece surface. Following which, the milling tool was set and clocked perpendicular to the machine spindle using a touch probe mounted upon the Y- translation stage. After accurately indexing the tool to 45 degrees via the B- rotary table, the tool was zeroed via contacting the corner of the workpiece. A coolant nozzle was also set near the machining zone with low pressure mist used to evacuate the chips. For this feasibility study, the machining parameters were set to a feed of 1000 mm/min and a rpm of 3000. With a DoC of 0.018 mm, the achievable lenslets would possess a length of 297.7 μm and a width of 265.9 μm.

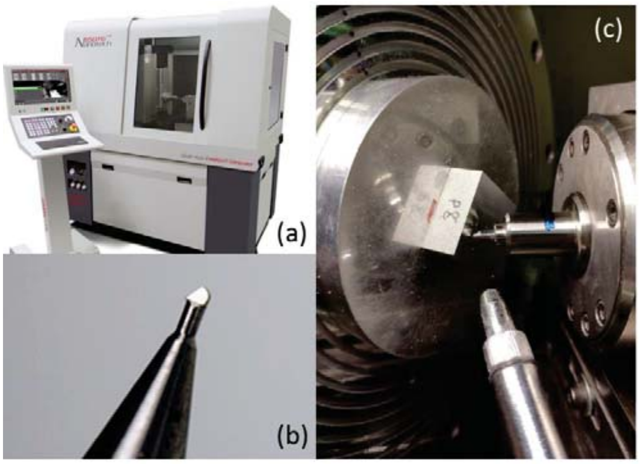

Fig. 6 (a) 5-axis Ultraprecision machine. (b) Diamond micromilling tool used in HESDM (c) Diagonal alignment of the tool to the workpiece surface.

3. Results and Discussion

Using the HESDM technique, the micro lens arrays were successfully machined upon the surface of the aluminum workpiece. To verify the geometry of the machined lenslets, optical measurements were done. As shown in Fig. 7, the length, and the width of the lenslets were measured to be 297.64 μm and 264.43 μm. Compared to the theoretical measurements, the deviations in the width could be attributed to tool deflection upon contact with the workpiece, while the length deviations can be due to the inaccuracy or instability of the milling spindle used.

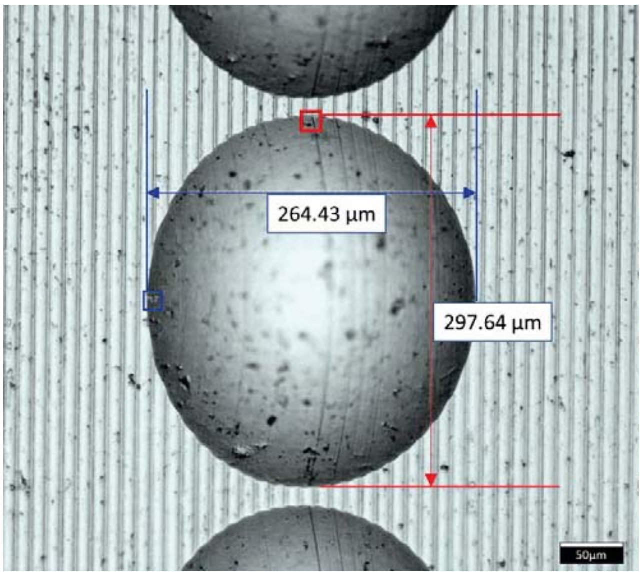

Fig. 7 Length and Width of micro lenslets generated using HESDM technique.

As for the surface finishing of the lenslets, a stylus profilometer was used to determine the quality of the lenses produced. Each lens possesses an Ra of 9.6~12.5 nm, with an average like that of conventional diamond turning techniques at of 11.2 nm, albeit with a much higher efficiency.

3. Conclusions (Times New Roman 10pt)

In this paper, the HESDM technique was successfully used to produce micro lenslet arrays using the synchronous relative motion of both the workpiece stage and a rotating diamond mill. Avoiding the need for non-productive indexing of the tool for each lens element, the synchronous motion rapidly generates the features along the tool path. Using a five-axis ultraprecision machine with a milling spindle mounted upon the rotational stage, the process was validated with the machining parameters set at a rpm of 3000, feed of 1000 mm/min and a DoC of 0.018 mm. The tool used was a 0.5 mm radii tool. The machined lenslets possess a length and width of 297.64 μm and 264.43 μm, which are slightly deviated from the theoretical values. These can be attributed to the inaccuracies and instability of the hardware. The surface finish of the lenslets measured an average of 11.2 nm, which can be considered optical quality.

ACKNOWLEDGEMENT

The authors would like to thank A*Star SIMTech for the support and resources to carry out this research.

REFERENCES

1. Andrews, J., Li, J., "Human Detection and Biometric Authentication with Ambient Sensors." In: Obeid, I., Picone, J., Selesnick, I. (eds) Biomedical Sensing and Analysis, Springer, Cham, 2002
2. Tan, N.Y.J., Zhang, X., Neo, D.W.K., Huang, R., Liu, K., and Kumar, A.S., "A review of recent advances in fabrication of optical Fresnel lenses," J. Manuf. Process, Vol. 71, pp. 113-133, 2021.
3. Tan, N.Y.J., Neo, D.W.K., Zhang, X., Liu, K., and Kumar, A.S., "Ultra-precision direct diamond shaping of functional micro features," J. Manuf. Process, Vol. 64, pp. 209-223, 2021.
4. Huang, R., Tan, N.Y.J., Neo, D.W.K., and Liu, K. "Reconfigured multi-axis diamond shaping of complex monolithic optics," CIRP Annals, Vol. 71, No. 1, pp. 69-72, 2022.
5. Zhang, X., Chen, Z., Chen, J., Wang, Z., and Zhu, L., "Fabrication of a microlens array featuring a high aspect ratio with a swinging diamond tool," J. Manuf. Process, Vol. 75, pp. 485-496, 2022.
6. Sato, Y. and Yan, J., "Tool path generation and optimization for freeform surface diamond turning based on an independently controlled fast tool servo" Int. J. Extreme. Manuf. Vol. 4, No. 2, 025102, 2022.